

Supplemental Data

Functional and Structural Analysis of the Siderophore Synthetase AsbB through Reconstitution of the Petrobactin Biosynthetic Pathway from *Bacillus anthracis*

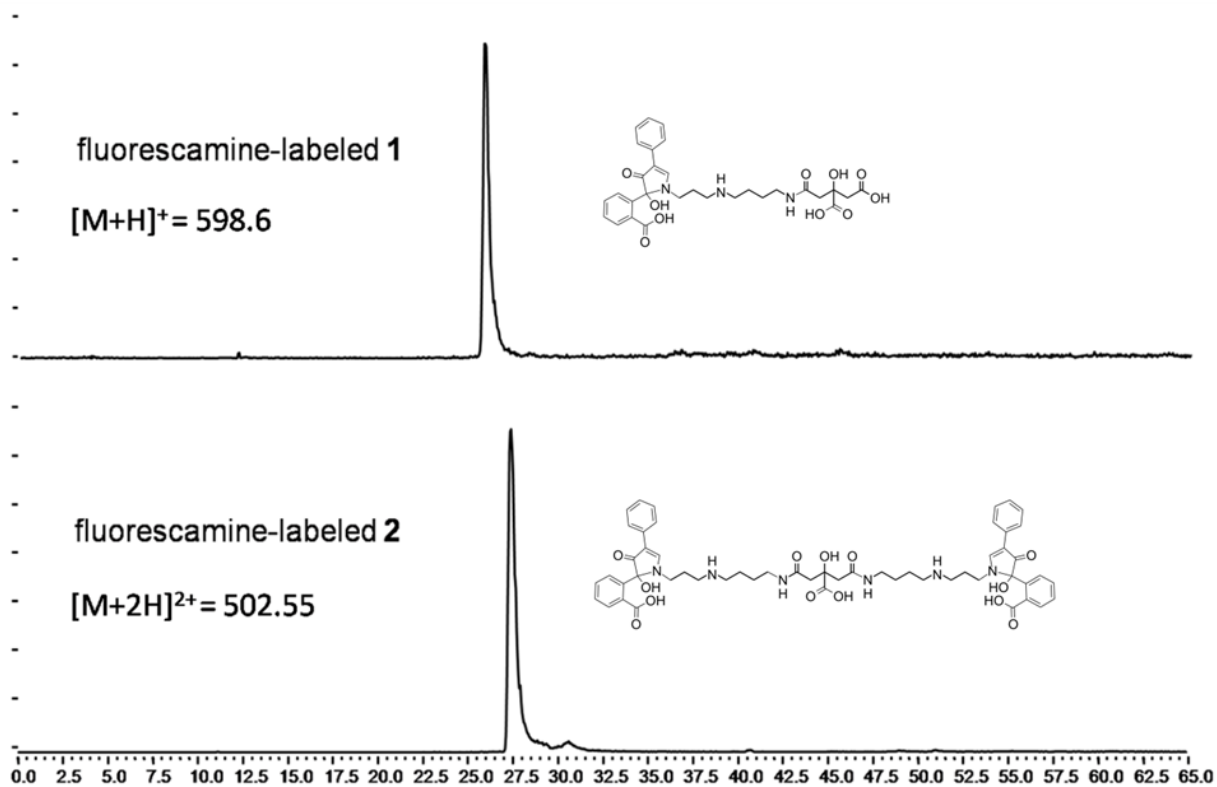
Tyler D. Nusca^{1,2†}, Youngchang Kim^{3†}, Natalia Maltseva³, William Eschenfeldt³, Lucy Stols³, Michael M. Schofield¹, Jamie B. Scaglione¹, Shandee D. Dixon², Daniel Oves-Costales⁴, Gregory L. Challis⁴, Philip C. Hanna², Brian F. Pflieger^{1,5}, Andrzej Joachimiak^{3,6}, and David H. Sherman^{1,2,7}

¹Life Sciences Institute and ²Department of Microbiology and Immunology, University of Michigan Medical School, Ann Arbor, Michigan 48109, USA, ³Midwest Center for Structural Genomics and Structural Biology Center, Biosciences Division, Argonne National Laboratory, 9700 South Cass Avenue, Building 202, Argonne, IL 60439, USA, ⁴Department of Chemistry, University of Warwick, Coventry CV4 7AL, UK, ⁵Department of Chemical and Biological Engineering, University of Wisconsin-Madison, 1415 Engineering Drive, Madison, WI 53706-1691, USA, ⁶Department of Biochemistry and Molecular Biology, University of Chicago, 920 E. 58th St., Chicago, IL 60637, USA, ⁷Departments of Medicinal Chemistry and Chemistry, University of Michigan, 210 Washtenaw Avenue, Ann Arbor, MI 48109, USA

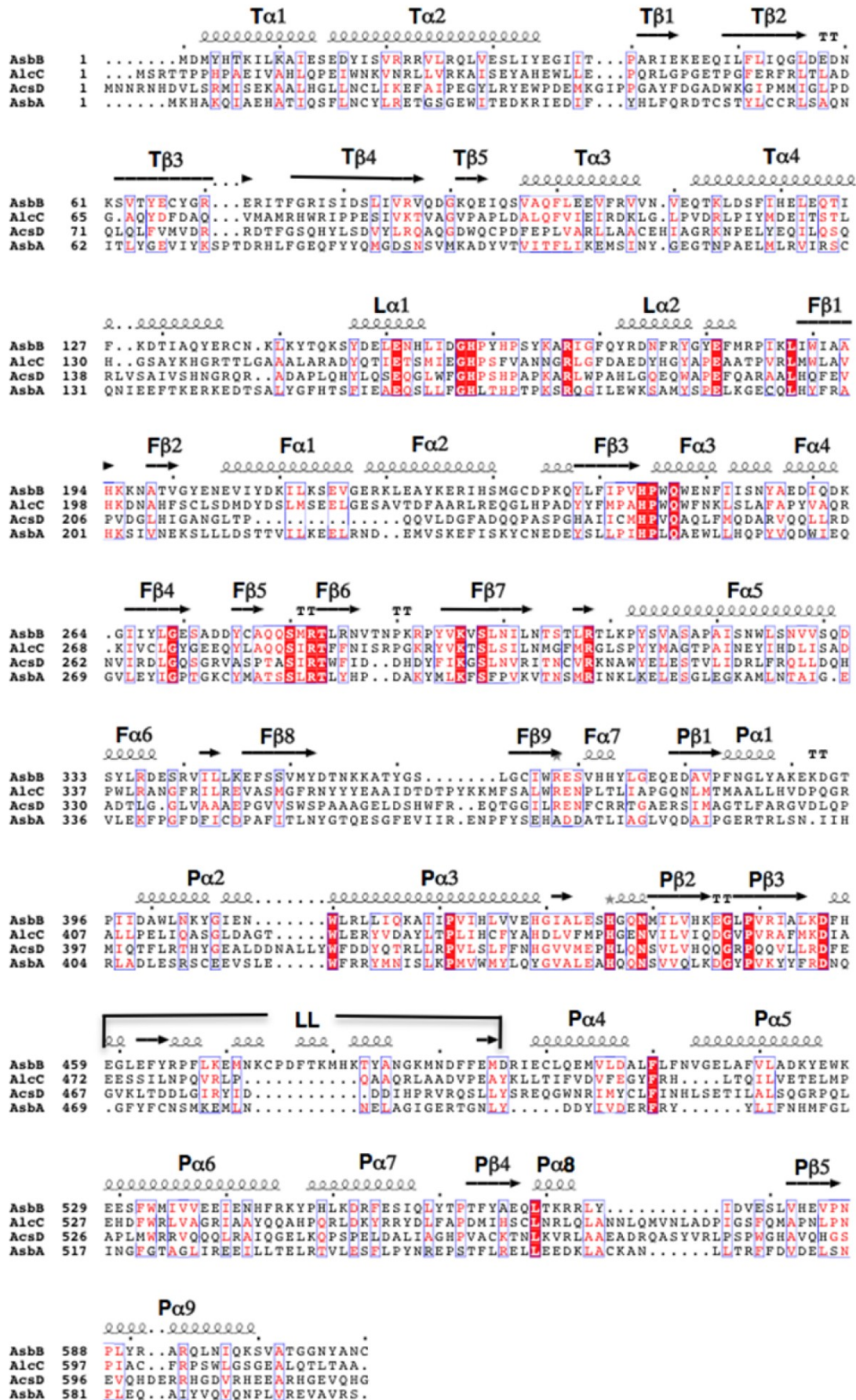
Contents:	Page:
Supplemental Table 1: Gene, vector, strain, and expression conditions.	S-2
Supplemental Figure 1: Fluorescamine derivatization of prepared standards.	S-3
Supplemental Figure 2: Sequence comparison of AsbB, AlcC, AcsD and AsbA.	S-4
Supplemental Figure 3: Modeling of ADP binding in the AsbB active site.	S-6
Supplemental Figure 4: Activity plots for quantitation of enzymatic efficiency.	S-7
Supplemental Figure 5: Reaction of AsbE with spermidine and 3,4-DHBA	S-8
Supplemental Methods: Protein Purification Techniques	S-10
References	S-10

Gene Name	Number	Expression Vector(s)	Cloning Strategy	Source	Antibiotic	Expression Strain
<i>asbA</i>	GBAA_1981	pMCSG26	LIC	this work	Amp, Spect, Tet	BLR (Invitrogen) cont. the pRARE plasmid (Novagen)
<i>asbB</i>	GBAA_1982	pET28b/pMCSG28	NdeI-XhoI/LIC	this work	Kan, Spect, Tet/Amp, Spect	BLR (Invitrogen)/ BL21 (DE3)-Gold (Invitrogen) cont. the pRARE plasmid (Novagen)
<i>asbC</i>	GBAA_1983	pET28b	NdeI-XhoI	ref. 4	Kan, Spect, Tet	BLR (Invitrogen)
<i>asbD</i>	GBAA_1984	pET28b	NdeI-XhoI	ref. 4	Kan, Tet/Kan	BLR (Invitrogen)/ BAP1 (Walsh Group, Harvard Univ)
<i>asbE</i>	GBAA_1985	pET28b	NdeI-XhoI	ref. 4	Kan, Tet	BLR (Invitrogen)

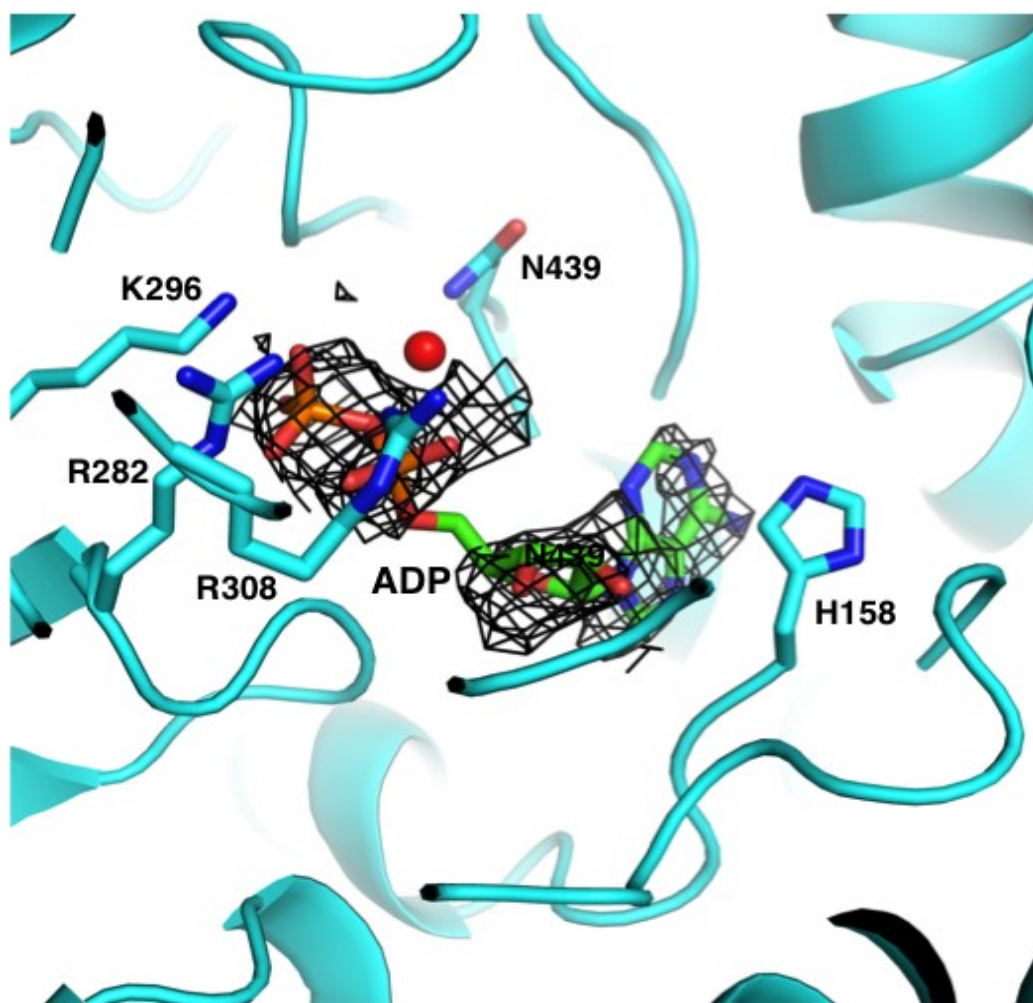
Supplemental Table 1. Gene, vector, strain, and expression conditions. LIC = Ligation independent cloning. Primer sequences and PCR conditions required for amplification of fragments is available upon request.



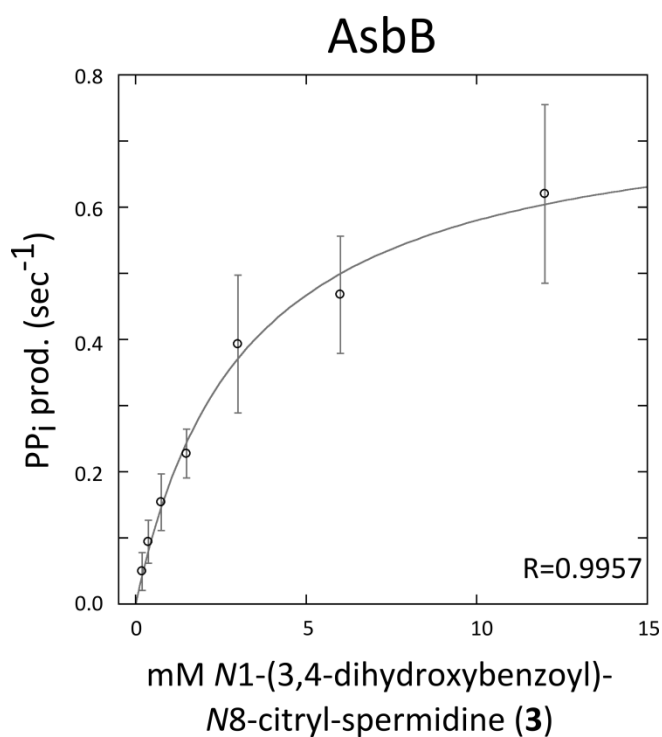
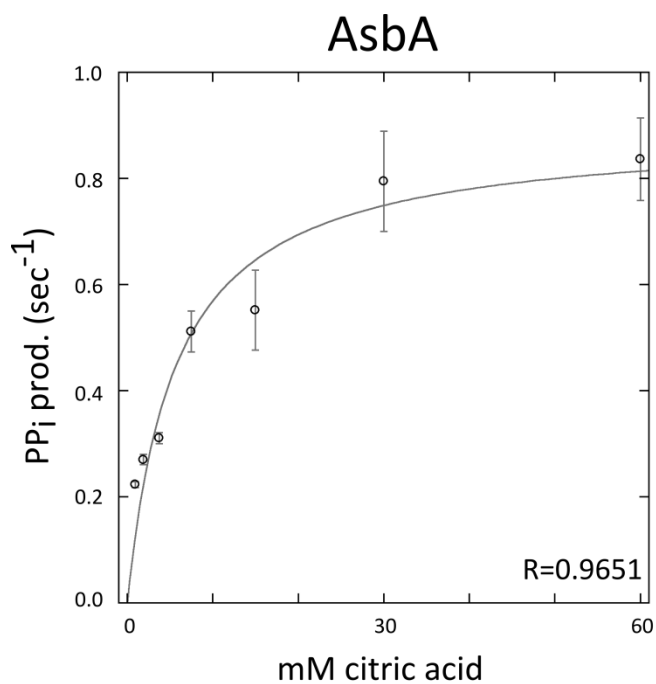
Supplemental Figure 1. Fluorescamine derivatization of prepared standards. Zwitterionic intermediates of petrobactin biosynthesis were derivatized with fluorescamine and analyzed by LC-MS using selected ion monitoring of predicted m/z of products.



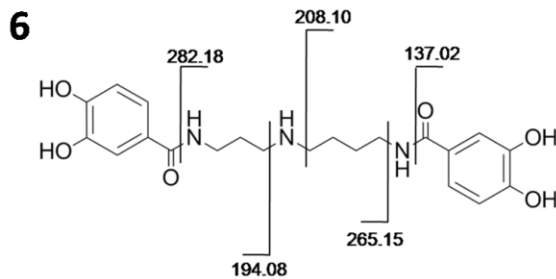
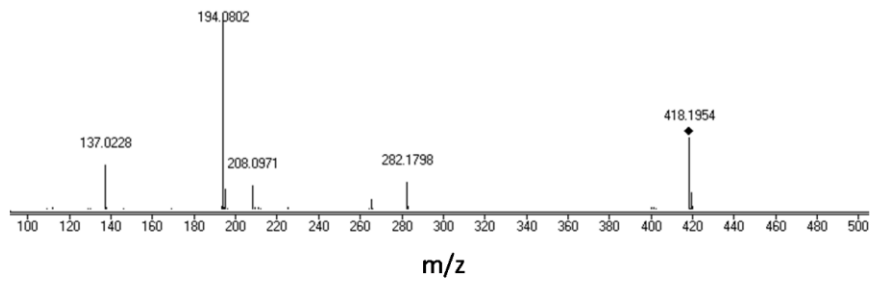
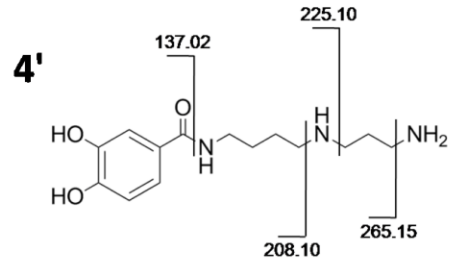
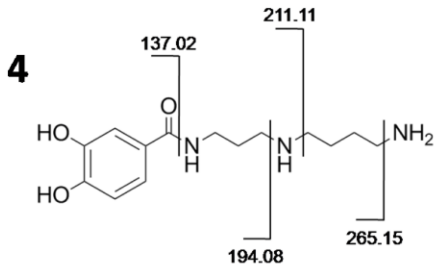
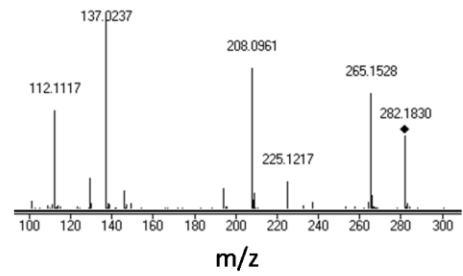
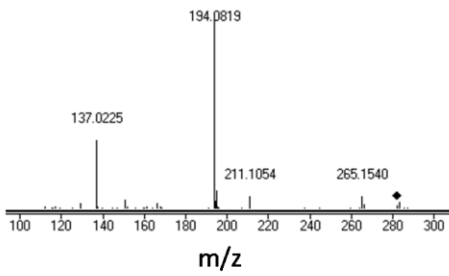
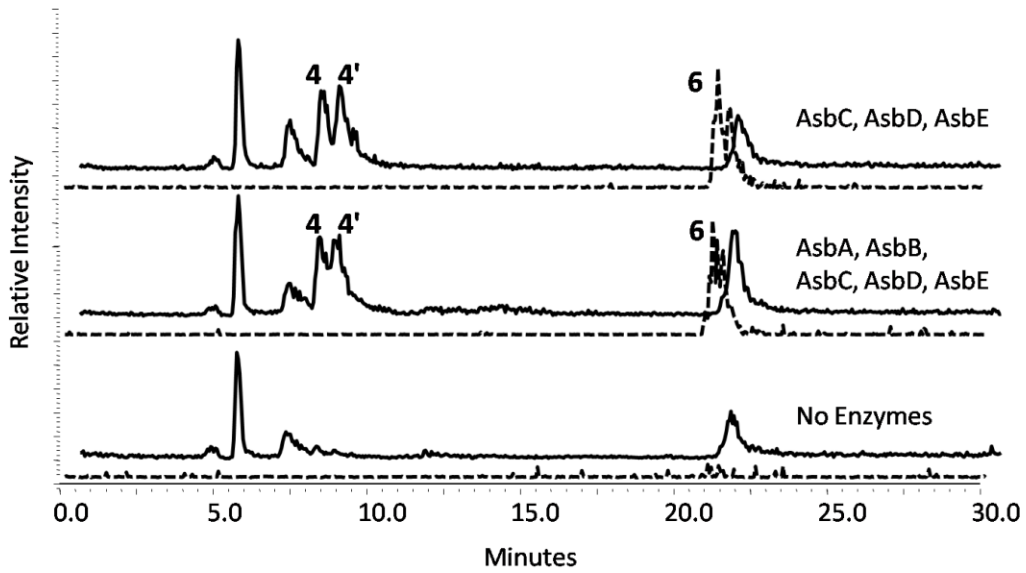
Supplemental Figure 2. Sequence comparison of AsbB, AlcC, AcsD and AsbA. The secondary structure of AsbB is annotated at the top. Highly conserved residues include H158, H161, R282, K308, E434, and N439 of AsbB. Hypothesized structural interactions with substrates are depicted in Fig. 3D.



Supplemental Figure 3. Modeling of ADP binding in the AsbB active site. ADP conformation is modeled and refined with partial occupancies based upon loose electron density data as demonstrated by the difference (Fo-Fc) electron density contoured at 3.0 σ (black mesh). Potential protein-substrate interactions are detailed in Figure 3D.



Supplemental Figure 4. Activity plots for quantification of enzymatic efficiency. His₆-AsbA and His₆-AsbB kinetic parameters were determined through plotting initial reaction rates over varying starting concentrations of adenylation substrate. The additional substrates of ATP and spermidine are at near-saturating levels of 6 mM and 40 mM, respectively. Reaction progress was monitored by observing release of pyrophosphate (PP_i) coupled to hydrolysis of the reporter molecule MESG to establish initial rates that were normalized to enzyme concentration. Only data-points not displaying substrate-associated background interference were used to extrapolate the curves. Nonlinear regression of these data using the Michaelis-Menten equation enabled prediction of V_{max} and K_m for approximation of V/K.



Supplemental Figure 5. Reaction of AsbE with spermidine and 3,4-DHBA. Initial reactions were analyzed by LC-MS as described in the text. Selective ion monitoring (SIM) was conducted in positive mode for predicted m/z of **4** and **4'** ($[M+H]^+=282.2$, solid traces). An extracted ion chromatogram (EIC) was rendered to detect compound **6** with a predicted m/z of $[M+H]^+=418.15$ (dashed traces). Corresponding peaks are observed in chromatograms of the petrobactin reconstitution enzymatic reaction and in instances where only the 3,4-DHBA - AMP ligase AsbC, the aryl-carrier protein AsbD, and the aryl transferase AsbE are the only proteins present. These results and previous research (1,2) suggest AsbC, AsbD, and AsbE are necessary and sufficient for formation of **4** and **4'** as well as **6**. The accumulation of these molecules during *in vitro* reconstitution of petrobactin biosynthesis (second trace) demonstrates a lack of incorporation into the final product petrobactin. Unlabeled peaks are consistently observed during LC-MS analysis of all reactions, including the no-enzyme control, and represent artifacts from the reaction. Predicted $[M+H]^+m/z$ of **4**, **4'**, and **6** were used to target corresponding species for MS/MS analysis. Fragmentation spectra confirm the 3,4-dihydroxybenzoylation pattern for all three compounds.

MS/MS settings are described in the main text. Injected reaction samples were separated on a Phenomenex Synergi Hydro-RP (150x4.6 mm, 4 μ m) column in-line with the instrument at a flow rate of 0.3 ml/min with mobile phase supplemented with 0.1% formic acid. 100% ddH₂O was applied for 5 minutes followed by a linear gradient of 0% to 95% MeCN over the course of 20 minutes. 95% MeCN was then applied for an additional 10 minutes.

Supplemental Methods

Protein Purification for Enzymology

All steps were conducted at 4°C. Briefly, harvested cell pellets were resuspended in 5 ml of lysis buffer (20 mM imidazole, 20 mM HEPES, 150 mM NaCl, 1 mM Tris(2-carboxyethyl) phosphine [TCEP], 10% v/v glycerol, pH 8) per 100 ml of original over-expression culture and lysed by sonication. Insoluble material was removed by ultracentrifugation at 30000 x g for 45 min, and the supernatant was batch-bound for 2 hours to 1 ml of Ni²⁺-NTA slurry (Novagen) that was previously equilibrated in lysis buffer. This batch-binding mixture was poured through a 5 ml fritted glass column where the retained resin was washed with 1 column volume of lysis buffer, 2 column volumes of wash buffer (40 mM imidazole, 20 mM HEPES, 150 mM NaCl, 1 mM TCEP, 10% glycerol, pH 8), and finally 3 ml of elution buffer (250 mM imidazole, 20 mM HEPES, 50 mM NaCl, 1 mM TCEP, 10% v/v glycerol, pH 8). Protein in the eluate was both exchanged into storage buffer (20 mM HEPES, 5 mM NaCl, 1 mM TCEP, 20% v/v glycerol, pH 8) and concentrated using Amicon Ultra centrifugal molecular weight cutoff filters (Millipore). Resulting samples were flash frozen with liquid N₂ and stored at -80°C prior to analysis.

Protein Purification for Crystallization

Harvested overexpression cells were lysed by sonication in the presence of 1 mg/ml lysozyme and a protease inhibitor cocktail tablet (Complete, Roche) in 35 ml of lysis buffer containing 50 mM HEPES pH 8.0, 500 mM NaCl, 10 mM imidazole, 10 mM β-mercaptoethanol, and 5% v/v glycerol. The lysate was clarified by centrifugation at 30000 x g for 75 min, followed by filtration through a 0.45 μm filter. Protein was purified by two-step Ni²⁺-affinity chromatography following the standard protocol described previously (3). Immobilized metal affinity chromatography (IMAC) was conducted using a 5ml HisTrap Chelating HP column charged with Ni²⁺ ions and buffer-exchange chromatography was performed on a HiPrep 26/10 desalting column (GE Healthcare) on an ÄKTExpress™ (GE Healthcare).

References

1. Lee, J. Y., Janes, B. K., Passalacqua, K. D., Pflieger, B. F., Bergman, N. H., Liu, H., Hakansson, K., Somu, R. V., Aldrich, C. C., Cendrowski, S., Hanna, P. C., and Sherman, D. H. (2007) *J. Bacteriol.* **189**, 1698-1710
2. Pflieger, B. F., Lee, J. Y., Somu, R. V., Aldrich, C. C., Hanna, P. C., and Sherman, D. H. (2007) *Biochemistry* **46**, 4147-4157
3. Kim, Y., Dementieva, I., Zhou, M., Wu, R., Lezondra, L., Quartey, P., Joachimiak, G., Korolev, O., Li, H., and Joachimiak, A. (2004) *J. Struct. Funct. Genomics* **5**, 111-118